Published in final edited form as:

Oncogene. 2014 July 24; 33(30): 3980–3991. doi:10.1038/onc.2013.367.

The Retinoblastoma Tumor Suppressor Pathway Modulates the Invasiveness of ErbB2 Positive Breast Cancer

Agnieszka K. Witkiewicz[1,2,*], **Derek W. Cox**[1], **Dayana Rivadeneira**[3], **Adam E. Ertel**[3], **Paolo Fortina**[3], **Gordon F. Schwartz**[4], and **Erik S. Knudsen**[1,2,*]

[1]Department of Pathology, UT Southwestern Medical Center, Dallas TX

[2]Simmons Cancer Center, UT Southwestern Medical Center, Dallas TX

[3]Department of Cancer Biology, Thomas Jefferson University, Philadelphia PA

[4]Department of Surgery, Thomas Jefferson University, Philadelphia PA

Abstract

The processes that control the progression of ductal carcinoma in situ (DCIS) to invasive breast cancer remain poorly understood. Epidermal growth factor receptor 2 (ErbB2) over expression is common in DCIS, as is disruption of the retinoblastoma tumor suppressor (RB) pathway. Here we examined the cooperative impact of ErbB2 and RB deregulation on facets of disease progression. Our studies demonstrate that RB deficiency altered the expression of key molecules needed for proper cellular organization and epithelial cell-cell adhesion as part of a program related to the epithelial to mesenchymal transition (EMT). An increase in the invasive potential of ErbB2 over expressing cells was observed upon RB depletion. Furthermore, stable knockdown of RB resulted in invasive lesions in orthotopic xenograft assays, compared to DCIS-like lesions developing from RB-proficient cells. Conversely, the invasive phenotype observed in ErbB2-positive cancer models was inhibited through CDK4/6 inhibition in an RB-dependent manner. Lastly, in a cohort of DCIS cases, we show that while elevated levels of ErbB2 are associated with increased risk of a subsequent DCIS recurrence, it is not associated with progression to invasive disease. In contrast, RB loss in ErbB2 positive DCIS cases was associated with increased risk for invasive breast cancer. Taken together, these data demonstrate a key role for the RB-pathway in invasion associated with breast tumor progression, and shed light on the key molecular events that promote the progression of DCIS to invasive disease.

Keywords

Tumor Suppressor; Epithelial to Mesenchymal Transition; Cyclin Dependent Kinase; Cell Cycle; E2F; CDK4/6; PD-0332991

Correspondence: Agnieszka K. Witkiewicz, Department of Pathology, UT Southwestern Medical Center, Dallas TX, agnes.witkiewicz@utsouthwestern.edu; Erik S. Knudsen, Department of Pathology, UT Southwestern Medical Center, Dallas TX, erik.knudsen@utsouthwestern.edu.

Introduction

A significant fraction of radiologically detected breast lesions are subsequently diagnosed as ductal carcinoma *in situ* (DCIS). With universal mammographic screening, the frequency of DCIS diagnosis has dramatically increased over the last twenty years (1, 2). While DCIS is generally associated with a favorable outcome, if left untreated, ∼40% of DCIS cases will progress to invasive disease that is potentially life-threatening (3). Therefore, veritably all patients diagnosed with DCIS are treated. Standard treatment for DCIS includes surgical resection of the lesion, typically followed by adjuvant radiation and/or or hormonal therapy (4, 5). Although effective at preventing the mortality associated with breast cancer, it is well appreciated that DCIS management could be improved (6). Due to an inability to efficiently stratify DCIS cases at high-risk of disease progression, many patients are treated with unnecessary adjuvant therapies that likely provide no clinical benefit (7-9). Conversely, a minor subset of DCIS recurs and progresses in spite of such interventions. Thus, there is a significant need to elucidate pathways that contribute to disease progression upon which to tailor therapeutic intervention.

The prognostic determinants of DCIS have lagged behind the detailed molecular analyses of invasive breast cancer (6). However, recent analyses of clinical specimens have revealed several features of DCIS that are associated with progression to invasive breast cancer (10, 11). Gene expression profiling from several groups comparing DCIS with invasive breast cancer has shown that a gene expression program associated with the epithelial to mesenchymal transition (EMT) is a unique property associated with invasive breast cancer (10, 11). These findings indicate that DCIS undergoing EMT would have a propensity to progress to invasive disease. Epithelial tissues are characterized by cytokeratins (CK), junctional complexes at cell-cell contact areas, and basal attachment to a basement membrane (12-14). These architectural components are important for epithelial cell homeostasis (15, 16), and the loss of such components as occurs during the process of EMT is associated with metastatic/invasive disease.

In parallel, with the molecular profiling analyses a number of studies have investigated specific oncogenic or tumor suppressive signaling proteins in DCIS. These targeted studies have utilized immunohistochemical or functional analysis to define pathways associated with the pathogenesis of DCIS. The ErbB2 oncoprotein is an important biomarker associated with advanced breast cancer classification, prognosis and therapeutic intervention (17-19). While ErbB2 over expression is observed in more than half of high-grade DCIS cases (20, 21), its prognostic value in DCIS is less clear. Studies of epithelial cell organization performed in three dimensional (3D) culture models have shown that ErbB2 over expression alone is not sufficient to induce cell invasion (22, 23). Correspondingly, ErbB2 over expression in DCIS has been associated with increased risk of disease recurrence, but not progression (24). Therefore, there are likely pathways that cooperate with ErbB2 to drive the progression to invasive disease. Amongst the pathways interrogated in DCIS, disruption of the retinoblastoma tumor suppressor (RB) pathway has been shown to be significantly associated with recurrence and disease progression of DCIS in multiple independent cohorts using different methodologies including direct staining and use of surrogate markers such as p16ink4a and Ki67 (24-27). RB is a key negative regulator of proliferation that links

multiple signaling pathways to the cell cycle machinery (28, 29). The RB-pathway is functionally disrupted in breast cancer by several mechanisms including the loss of heterozygosity at the *RB1* locus in ErbB2 over expressing breast cancer subtypes (30, 31). Taken together, these studies suggest a potential role for the cooperation between RB loss and ErbB2 over expression in specifically driving DCIS progression.

Results

Loss of RB and ErbB2 over expression results in deregulated mammary cell proliferation and acinar growth

In order to interrogate the individual and combined effect of RB loss and ErbB2 over expression, we utilized the immortalized mammary epithelial cell line MCF10A. Stable polyclonal RB-knockdown MCF10A cell line (MCF10A miRB) and scrambled control cell line (MCF10A miNS) are shown in Figure 1A. Biochemical analysis of the expression of downstream RB/E2F target genes (Cyclin A and MCM7) demonstrated minimal differences in protein expression from cells grown in culture as a monolayer (Figure 1A, top panel), as well as minimal change in proliferation as shown by BrdU incorporation (Figure 1A, bottom panel). To interrogate the phenotypic effects of pathway perturbation on the glandular organization of mammary epithelia, 3D cultures were employed (32, 33). RB-proficient MCF10A cells (miNS) generated normal acinar structures displaying growth arrest by 10 days as depicted by Ki67 staining. In contrast, RB-deficient cells showed approximately a 30% proliferation rate even after 10 days of culture (Figure 1B). To investigate the impact of RB loss in the context of ErbB2 over expression, we over expressed ErbB2 in RB-deficient MCF10A cells as shown in Figure 1C. These cultures exhibited similar levels of ErbB2 as observed in ErbB2 positive breast cancer cell lines, and demonstrated relatively uniform loss of RB throughout the culture as determined by immunofluorescence microscopy (Supplemental Figure 1). Similar to results displayed in Figure 1A, RB depletion resulted in minimal alterations in the expression of RB/E2F target genes (Cyclin A, MCM7) in ErbB2 over expressing MCF10A cells, and proliferation rates remained virtually unchanged compared to RB-proficient cells (Figure 1C). In the presence of ErbB2 over expression, RB-proficient and RB-deficient acinar structures exhibited similar proliferation rates as determined by Ki67 staining (Figure 1D). Thus, in the context of proliferation, loss of RB has little impact over that observed by ErbB2 over expression alone.

Combinatorial effect of ErbB2- and RB-pathways on acinar morphology

While RB-deficiency had little impact on the proliferation of ErbB2 over expressing mammary cells, a noticeable impact on the morphology of the acinar structures was observed (Figure 2A). RB-proficient and RB-deficient cells generated spherical acini with a hollow lumen, and well-organized actin expression throughout the epithelial cells as determined utilizing phalloidin staining (Figure 2A, top left panels). Consistent with the enhanced proliferation observed with RB loss in MCF10A acini, an increase in acini volume was observed (Figure 2A, bottom left panel). However, as previously shown (22), ErbB2 over expressing MCF10A cells displayed a multi-acinar phenotype and absence of a hollow lumen (Figure 2A, top right panels). Consistent with the minimum difference in proliferation rates, minimal difference in acinar volume was observed with RB-deficiency in cells

expressing ErbB2 (Figure 2A, bottom right panel). However, the combined perturbation of the ErbB2- and RB-pathways resulted in further disorganization of the structures, with the appearance of “stellate” acinar morphology as shown by phase contrast images (34), with cellular protrusions escaping from the acinar structure into the surrounding matrigel (Figure 2A, right panels). The appearance of aberrant invasion into the surrounding matrix could be observed as early as 3 days post-plating (not shown), and was clearly apparent within 6 days (Figure 2B).

Gene expression profiling defines impact of RB deficiency on features of epithelial biology and invasion

To define how RB loss influences the acinar morphology of ErbB2 over expressing cells, gene expression profiling of RB-proficient and RB-deficient ErbB2 over expressing MCF10A cells grown in 3D cell culture was performed (Figure 2C). These data revealed a significant number of genes that were reproducibly up and down regulated with RB depletion (Supplemental Table 1). Amongst down-regulated genes there were a substantial number of genes associated with epithelial differentiation, cell-cell adhesion, and tissue function. Gene set enrichment analysis (GSEA) was utilized to compare the genes defined in our microarray analysis to previously described EMT core gene expression signature that is specifically associated with invasive breast cancer vs. DCIS (35). The data from the combined deregulation of the ErbB2- and RB-pathways showed a strong overlap ($p<1E-5$) with this EMT core signature (Figure 2C, middle panel) and revealed a significant decrease in the expression of multiple epithelial markers (*KRT18*, *KRT15*, *KRT17*) and structural and cell adhesion molecules important for epithelial architecture (*ITGB4*, *JUP*, *DSG1*, *SFN*) (Figure 2C, right panel). Thus, RB loss has a significant impact on the acinar morphology of ErbB2 overexpressing cells and alters the expression of molecules implicated in EMT.

Loss of epithelial characteristics and impact of RB loss on polarity

To functionally validate the gene expression data, western blotting and immunofluorescence microscopy was performed. As shown, there was significant down-regulation of multiple cytokeratins at the protein level with RB-knockdown in ErbB2-expressing MCF10A cells (Figure 3A). There was a concordant reduction in cytokeratin expression as determined by fluorescence microscopy in 2D cultures (Figure 3B). These findings were also apparent in 3D cultures (Figure 3C). Correspondingly, junctional plakaglobin (JUP), which is a critical adhesion molecule, was significantly reduced consistent with the gene expression analyses (Figure 3D). While the levels of E-Cadherin were only modestly reduced as determined by microarray; there was a deficit in E-Cadherin expression/localization that was apparent in disorganized acinar structures at and the leading edge of ErbB2-positive and RB-deficient cells grown in 2D (Figure 3D). Together these data indicate that there is substantial decrease in the expression of key epithelial specific proteins that are important for tissue architecture and invasion. An important characteristic of normal acini is the deposition of basement membrane components such as Laminin V (36). While uniform basal Laminin V expression was displayed around RB-proficient ErbB2 over expressing acini, RB-deficient ErbB2 over expressing cells harbored diffuse Laminin V expression throughout the acini, indicating disruption of cellular polarization (Figure 3E). Taken together, these data indicate that upon RB loss in ErbB2 over expressing cells, there is a disruption of cell polarity and defective

cell-cell junction complexes through both changes in gene expression and molecule localization that could lead to the deregulation of key cellular functions such as cell motility.

RB loss promotes invasive properties in ErbB2 expressing mammary epithelial cells and breast cancer cell lines

To determine if RB-deficiency had an effect on cell motility, the migratory and invasive activity of RB-proficient and RB-deficient ErbB2 over expressing cells was assessed by Boyden chamber assays. While loss of RB or over expression of ErbB2 alone was observed to increase the migratory ability of MCF10A cells, the combined deregulation of the ErbB2- and RB-pathways demonstrated a cooperative enhancement of cell migration (Figure 4A). Upon examination of cell invasion, we found that while RB loss alone had minimal impact on the invasive potential of MCF10A cells, ErbB2 over expression significantly increased cell invasion (Figure 4B). Furthermore, combined deregulation of the ErbB2- and RB-pathways resulted in an ∼2-fold increase in cell invasion over ErbB2 over expression alone. These effects were dependent on downstream signaling through the ERK and AKT pathways. Specific pharmaceutical inhibition of AKT had a dramatic impact on invasion of all cells, while inhibition of ERK signaling had a particular impact on RB-deficient models (Supplemental Figure 2). These results suggest that RB-deficiency contributes to a more invasive phenotype in ErbB2 expressing mammary epithelial cells.

To determine whether the impact of RB loss on cell invasion was also relevant in established ErbB2 positive breast cancer models, we generated RB-deficient SKBR3 and BT474 cell lines as shown in Figure 4C and 4D. Consistent with results observed in the MCF10A models, RB loss resulted in only a slight increase in RB/E2F target genes protein expression (MCM7, Cyclin A, PCNA) and cell proliferation as demonstrated by BrdU incorporation in both cell lines (Figure 4C, D). However, despite the minimal effects on proliferation, a significant increase was observed in cell migration (Figure 4E) and cell invasion (Figure 4F) in both RB-deficient SKBR3 and BT474 cells. These data indicate that RB loss can enhance cell migration and invasion in ErbB2 positive breast cancer cells.

Pharmaceutical activation of the RB-pathway prevents abnormal multi-acini growth and cell invasion

Our data indicate that RB loss cooperates with ErbB2 in promoting invasive behavior. To investigate whether activation of the RB-pathway could have an inhibitory effect on the invasive phenotype observed with ErbB2 over expression, we used a highly specific CDK4/6 inhibitor PD-0332991 (PD) (37, 38). The ability of PD0332991 to decrease RB/E2F gene expression and inhibit cell proliferation in MCF10A cells has been previously established (39). As shown in Figure 5A, inhibition of CDK4/6 was exceedingly effective at repressing RB/E2F gene expression (MCM7, Cyclin A, PCNA) and cell proliferation even in cells harboring ErbB2 over expression. This inhibition of proliferation was observed in both 2D and 3D cell cultures (Figure 5A). Interestingly, CDK4/6 inhibition was also effective at preventing the formation of multi-acini structures in 3D culture (Figure 5B, left panel), and significantly inhibited cell invasion (Figure 5B, right panel). These effects were dependent on RB status as shown by the minimal effect of PD0332991 on invasive phenotype of RB-deficient cells (Figure 5B, right panel).

To determine if CDK4/6 inhibition could be effective in inhibiting proliferation of RB-proficient, ErbB2 over expressing breast cancer populations, we analyzed the effects of PD0332991 on BT474 cells. Indeed, CDK4/6 inhibition significantly decreased RB/E2F target gene expression, as well as cell proliferation of BT474 cells in both 2D and 3D culture (Figure 5C). Importantly, PD-0332991 treatment dramatically inhibited the formation of abnormal acini structures, and repressed cell invasion in an RB dependent manner (Figure 5D). Combined, these data suggest that targeting the RB-pathway could be a potential therapeutic option for the treatment of ErbB2 over expressing breast cancer limiting both proliferation and the ability of such cells tumors to invade.

RB plays a role in limiting invasive progression *in vivo*

Several commonly utilized breast cancer cell lines have been classified as weakly invasive, such as ZR75-1, MDA-MB-453, and SKBR3 cells (40). To examine the ability of RB loss to enhance the invasive potential of ErbB2 over expressing breast cancer cells *in vivo*, we injected RB-proficient and RB-deficient ErbB2-positive SKBR3 cells into the mammary fat pad of ten-week-old NOD/SCID mice. This model system gave rise to ErbB2 over expressing DCIS lesions after six months (Figure 6A). Smooth muscle actin (SMA) and ErbB2 staining was used to demonstrate ErbB2 over expressing DCIS lesions confined by a continuous myoepithelial layer (Figure 6A). Importantly, this confined structure was dependent on the presence of RB, as RB-deficient SKBR3 lesions displayed an invasive phenotype as indicated by the poorly defined SMA expression (Figure 6A and 6B) and invasion of proliferative cells into the surrounding stroma (Ki67, Figure 6B). Consistent with our *in vitro* analyses, no difference in proliferation was observed between the RB-proficient and RB-deficient lesions (*Ki67*, Figure 6B), indicating that the impact of RB loss in the context of ErbB2 over expression is predominantly associated with cell adhesion and epithelial cell motility.

RB deficiency modifies the risk of recurrence and progression in Her2-positive DCIS

The observation that RB-deficiency is associated with enhanced invasive properties and cooperated with ErbB2 over expression, supported a combined role for the two pathways in DCIS progression. We employed a cohort of 226 cases of DCIS for which ErbB2 and RB status were determined. These patient that were treated with surgery in the absence of adjuvant therapy, with long-term followup (median 8.6 years)(26). This cohort provides the opportunity to specifically evaluate prognostic markers of ipsilateral breast events or invasive progression. Optimized staining for ErB2 and RB was performed (representative images, Figure 7A). Consistent with other studies (41), elevated ErbB2 expression (3+ staining) is observed in DCIS and is associated with a modest increase in risk for subsequent DCIS recurrence (Figure 7B). However, overexpression of ErbB2 is not associated with increased risk for invasion ($p>0.05$). In ErbB2-positive DCIS, histochemical RB loss was observed in approximately 25 percent of cases. In this setting RB loss was associated with a further increased risk for recurrence within ErbB2-positive and importantly was also significantly associated with progression to invasive breast cancer (Figure 7C). These data, suggest that loss of RB can contribute to the function of ErbB2 in driving disease progression.

Discussion

Breast cancer is a complex and heterogeneous collection of disease conditions. While sophisticated treatment approaches are employed in the context of invasive disease; there is significant uncertainty related to how to best treat DCIS (6, 24, 42-44). Surgical resection coupled with adjuvant therapy, is the mainstay of therapy with little consideration of underlying pathways that may be relevant to disease course and risk of progression to invasive breast cancer. Here we evaluated the cooperative impact of ErbB2 and RB pathways that are frequently dysregulated in DCIS.

Work from multiple groups has shown that ErbB2 has an important impact on the biology of mammary epithelial cells. In 3D cultures, ErbB2 promotes both proliferation and cellular survival leading to filled acinar structures that exhibit specific architectural alterations (22, 32). In spite of these potent effects, and consistent with our observations reported here, ErbB2 is not sufficient to drive invasion into the surrounding matrix. RB-deficiency had relatively modest effects on the proliferation of mammary epithelial cells, and they still exhibited apoptosis leading to hollow acinar structures; however, RB-deficiency potently cooperated with ErbB2 loss. Most strikingly, RB-deficiency allowed mammary epithelial cells to rapidly invade out of the 3D structure and away from the primary acinus, leading to a stellate morphology. This finding was not associated with a significant increase in proliferation; underscoring a non-canonical function for RB loss in this setting. Gene expression profiling revealed a significant change in expression of a number of cellular components involved in cell-cell adhesion and cellular architecture. GSEA analysis showed a strong overlap between the genes down-regulated in RB-deficient ErbB2 over expressing cells and the EMT core signature generated by Dr. Weinberg's group (35). It is widely accepted that in order to activate invasion and metastasis, disruption of the cellular architecture, cell-cell adhesions and cell polarity must occur (45, 46). It should be noted that the molecular changes observed in our models, most recapitulate loss of an epithelial phenotype as opposed to full EMT as there was not a concomitant increase in mesenchymal gene expression. However, there were significant parallels between the findings from our *in vitro* studies, and the finding that a key difference between DCIS and invasive breast cancer is an EMT gene expression program(47).

Paramount to disease progression in breast cancer, is the ability for the cancer cells in DCIS to invade out of the duct into the surrounding stroma. The biology surrounding this feature of disease is under intense scrutiny, and likely reflects a number of acquired mutations/ epigenetic alterations in the DCIS lesion. ErbB2 is noted for promoting proliferation and invasion; however, invasive effects were strongly augmented by RB knockdown in 3D culture and Boyden chamber assays. This activity of RB was blocked by both ERK and AKT inhibition, indicating that there is a specific dependency on these signaling pathways. While distinct cells invaded out of acinar structures, analyses of AKT signaling by immunostaining of 3D cultures did not indicate that such cells were particularly deregulated for ErbB2-mediated signaling (not shown). Importantly, RB loss had a significant impact on the characteristics of ErbB2-positive tumor cell growth in orthotopic models, where it facilitated dissemination in to the stroma of the mammary gland. These findings would suggest a functional role for RB and ErbB2 in disease progression. This supposition was

supported by the analyses of DCIS cases with long-term followup. In this context, ErbB2 is a determinant of recurrence, but is not associated with disease progression. However, in ErbB2 positive DCIS, RB loss was associated with further increased risk of recurrence but uniquely invasive progression. These findings suggest that composite low ErbB2 and positive RB status could be useful for delineating DCIS at low-risk for recurrence/progression that could be treated by surgery alone.

Disruption of the RB pathway is likely an important factor contributing to progression of ErbB2 over expressing DCIS. In many contexts, RB inactivation is mediated through the action of cyclin D1 which is frequently over expressed and amplified in breast cancer (48). Thus, pharmacological inhibition of cyclin D-associated kinase activity could represent an effective means to repress proliferation of such lesions. Our group and others have demonstrated the efficacy of reactivating RB function and cell cycle arrest in various types of cancer, including breast cancer, through pharmacological CDK4/6 inhibition (49, 50). In the present study, exposure to the CDK4/6 inhibitor PD-0332991 induced a potent cell cycle arrest among RB-proficient, ErbB2 positive cancer cells. Since this is a cytostatic compound, it is crucial to delineate its influence on possible tumor spread. Treatment with PD-0332991 inhibited the invasive properties of ErbB2-positive models in Boyden chamber and 3D culture, which was largely dependent on RB. Presently, PD-0332991 is undergoing phase II/III evaluation in ER positive breast cancer. Thus, for women presenting with Erb2 positive disease PD-0332991 could represent a means to both repress cell proliferation and invasion associated with progression to advanced disease.

The present study demonstrates that loss of RB function can have a significant impact in disease progression in ErbB2 positive breast cancer by disrupting normal epithelial cell architecture and organization. Additional studies with independent DCIS cohorts are needed to further validate the prognostic value of RB-pathway disruption in ErbB2 over expressing DCIS cases. Furthermore with the emergences of next generation CDK4/6 inhibitors, RB-pathway analysis will allow for stratification of patients that are likely to respond to novel target therapies. Overall our study shows that the RB-pathway plays an important role in Erbb2 positive disease and could be utilized as a biomarker for invasive disease and target for novel therapeutic regimens.

Materials and Methods

Cell culture

MCF10A cells were maintained in DMEM/F12 supplemented with 5% Horse Serum, 20ng/ml EGF, 10ug/ml insulin, 1ng/ml cholera toxin, 100ug/ml hydrocortisone, 100U/ml penicillin/streptomycin and 2mM L-glutamine. BT474 cells were propagated in DMEM containing 10% FBS supplemented with 100 U/ml penicillin/streptomycin and 2mM L-glutamine at 37°C and 5% CO_2. SKBR3 cells were propagated in RPMI containing 10% FBS supplemented with 100 U/ml penicillin/streptomycin and 2mM L-glutamine at 37°C and 5% CO_2.

Viral expression plasmids and infections

pMSCV-LMP-miRB and pMSCV-LMP-miNS vectors were used to generate *Rb*-targeting (miRB) or non-specific control (miNS) recombinant retroviruses as previously described (49). pDONR223-ERBB2 was a kind gift from Dr. Andrew Aplin (Thomas Jefferson University). Plasmid was originally purchased from Addgene (plasmid 23888) and recombined using LR Clonase II from Invitrogen into pLenti6/UbC/V5-DEST from Invitrogen to generate pLenti6/UbC/V5-GW/ERBB2. pLenti6/UbC/V5-GW/lacZ was purchased from Invitrogen. Retroviral infections of MCF10A, SKBR3 and BT474 cells were performed as previously described (39). Lentiviral infection was done by incubating MCF10A cells with ErbB2 lentivirus for 48 hours. Non-infected cells were eliminated by selection with G418.

Drug Treatments

The specific CDK4/6 inhibitor PD-0332991 (PD) was used as previously described (37, 38). Stock solutions of PD (100μM) were prepared in dimethyl sulfoxide (DMSO) and cells were treated with the 1μM PD for times indicated.

BrdU labeling and bivariate flow cytometry

For cell proliferation analysis cells were incubated with bromodeoxyuridine (BrdU) (Amersham Pharmacia Biotech) for one hour before harvest. Cells were washed in PBS, fixed in cold 70% ethanol and bivariate flow cytometry was utilized for dual analysis of BrdU incorporation and total DNA content as previously described (51).

Immunoblot Analysis

Equal total protein was resolved by SDS-PAGE. Proteins were detected by standard immunoblotting procedures using the following primary antibodies: hCyclin A (H432), RNR2 (I-15), MCM7 (141.2), PCNA (PC10), ErbB2 (SP3, Freemont, CA, USA), Lamin B (M-20) (Santa Cruz Biotechnology, Santa Cruz, CA, USA), RB (G3–245) (Becton Dickson, Franklin Lakes, NJ, USA,).

Three-Dimensional (3-D) Cultures of Mammary Epithelial Cells

Cells were treated with trypsin and resuspended in Assay medium (DMEM/F12 supplemented with 2% horse serum, 10μg/ml insulin 1ng/ml cholera toxin, 100μg/ml hydrocortisone, 100 U/ml penicillin/streptomycin and 2mM L-glutamine at a concentration of 25,000 cells per ml. Eight-chambered RS glass slides (Nalgene Nunc. Naperville, IL) were coated with 40μl Matrigel (BD Bioscience Bedford, MA, USA) and solidified for 30 min. The cells were mixed 1:1 with assay medium containing 4% Matrigel and 10ng/ml EGF. 400μl of cells mixture was added to each well with 5,000 cells per chamber. Assay media was replaced every 4 days.

Quantification of Mammary Acini Growth

Acini growth was monitored by imaging MCF10A miNS and MCF10A miRB acini using an Olympus 80X microscope with a 10X objective connected with a cooled charge-coupled device camera. Diameters were measured at the middle optical section of each acinus, with

the support of Image J software. A minimum of 50 acini were scored for each genotype. Volume was calculated using the acquired diameter and the formula ($4/3\pi r^3$).

Immunofluorescence analysis

Immunofluorescence staining of acini was performed as previously described (52). For details on antibodies refer to table in supplemental material and methods. Staining in 2D was performed on methanol fixed cells using the antibodies summarized in the supplemental materials.

Migration and Invasion Assays

MCF10A cells were seeded (5×10^4 cells) on Boyden Chambers (Franklin Lakes, NJ; BioCoat 354578) under low serum conditions. Complete growth medium was added to the wells as the chemo-attractant. Chambers were placed in wells containing complete medium. The cells on the lower surface of the membrane were counterstained with 4,6-diamidino-2-phenylindole (DAPI) (Sigma-Aldrich, St. Louis, MO, USA). Cells were scored with a fluorescent microscope.

RNA extraction from 3D acini cultures

Media was aspirated from 8-well chamber-slides and added 250 μl of RNA-STAT-60 (Tel-Test, Friendswood, TX, USA) to each well. Immediately the mixture of cells and matrigel was resuspended several times and collected in an Eppendorf tube. Following steps were followed according to manufacturer's instructions.

Microarray sample preparation and hybridization

RNA was quantified on a NanoDrop spectrophotometer, followed by RNA quality assessment on an Agilent 2100 bioanalyzer (Agilent, Palo Alto, CA, USA). Amplification of cDNA was performed using the Ovation Pico WTA-system V2 RNA amplification system (NuGen Technologies, Inc.). Briefly, 50 ng of total RNA was reverse transcribed using a chimeric cDNA/mRNA primer, and a second complementary cDNA strand was synthesized. Purified cDNA was then amplified with ribo-SPIA enzyme and SPIA DNA/RNA primers (NuGEN Technologies, Inc.). Amplified ST-cDNA was purified with Qiagen MinElute reaction cleanup kit. The concentration of Purified ST-cDNA was measured using the Nanodrop. 2.5 μg ST-cDNAs were fragmented and chemically labeled with biotin to generate biotinylated ST-cDNA using FL-Ovation cDNA biotin module V2 (NuGen Technologies, Inc.).

Affymetrix GeneChip Human Gene 1.0 ST arrays (Affymetrix, Santa Clara, CA), were hybridized with fragmented and biotin-labeled target (2.5 μg) in 110 μl of hybridization cocktail. Target denaturation was performed at 99°C for 2 min. and then 45°C for 5 min, followed by hybridization for 18 h. Arrays were then washed and stained using Gene chip Fluidic Station 450, and hybridization signals were amplified using antibody amplification with goat IgG and anti-streptavidin biotinylated antibody. Chips were scanned on an Affymetrix Gene Chip Scanner 3000, using Command Console Software.

Microarray Normalization

Raw data files from the Affymetrix GeneChip Human Gene 1.0 ST arrays were processed using Affymetrix Expression Console version 1.1. Gene-level expression measurements were computed using the iterPLIER algorithm on the “core” probesets and exported with annotation release 32, dated June 23rd, 2011. Additional array preprocessing was performed in Matlab version 7.13.0 (R2011b), where expression values were converted to iterPLIER +16 by adding 16, and then transformed to log2 scale. Prior to analysis, data was filtered to exclude probesets with no gene annotation, and genes with multiple probesets were handled by averaging their rows together and scaling by the probeset with the largest standard deviation. Additional data filtering and differential expression analysis were performed in matlab.

Differential expression analysis

Differential gene expression analysis expression analysis between sample conditions samples was using a two-sample t-test with unequal variance. 10000 sample permutations were performed for improved p-value estimations. To account for multiple testing, p-values were adjusted based on the estimated false discovery rate (FDR), using the procedure introduced by Storey, 2002 (53). For increased statistical power, genes with variance below the 50^{th} percentile or expressed below the 25^{th} percentile in over 90% of the samples being compared were assigned an adjusted p-value of 1 and filtered out prior to false discovery rate estimation (54). Differentially expressed genes were identified as those with an adjusted FDR ≤ 0.25 and minimum 1.5 fold change.

Gene set enrichment analysis

A collection of previously described gene sets was analyzed for enrichment in ErbB2-overexpressing miRB cells. Specific gene sets include epithelial-to-mesenchymal transition genes reported in Taube 2010 (35). The Gene Set Enrichment Analysis (GSEA) software tool (55) was used to identify similarities between expression profiles in our microarray dataset the previously reported disease progression/invasion gene sets.

Mammary fat Pad injections, histology and immunohistochemistry

Mammary gland tissue was embedded in paraffin and sectioned at 4 μm. Tissue sections were deparaffinized in xylene and rehydrated through an ethanol gradient. For histological analysis, tissue sections were stained in hematoxylin and eosin (H&E) using standard staining techniques. Immunohistochemistry was performed as previously described (56). Experiments were conducted in accordance with the NIH Guide for Care and Use of Laboratory Animals and approved by the Thomas Jefferson University Institutional Animal Care and Use Committee. For orthotopic injections mice were anesthetized with the use of Isoflourane. We then performed a Y-incision on the abdomen in order to expose the inguinal gland. 5×10^6 cells were resuspended in 100 ul of PBS and injected in the left mammary fat pad. Incisions were closed and mice were monitored every week.

DCIS patient cohort and immunohistochemistry

The DCIS cohort was developed from patients who underwent surgical resection from 1978 to 2008, with median 8.6 years follow up. Detailed demographic information has been previously described. Cases were included for whom tissue was available for staining with both ErbB2 and RB. ErbB2 staining (clone 4B5) was performed on the BenchMark XT Slide Preparation System following the manufacturer's guidelines (Ventana Medical Systems, Tucson, AZ). RB was stained by employing a standard immunoperoxidase method (dilution 1:50, clone 1F8, Thermoscientific).

Statistical Analyses

Statistical analyses were performed with GraphPad Prism software (La Jolla, CA). *P*- values were calculated by performing Student t tests. $P < .05$ was considered significant.

Supplementary Material

Refer to Web version on PubMed Central for supplementary material.

Acknowledgments

The authors would like to thank all of their colleagues who contributed to this study. This work was supported by NIH grants to ESK (RO1-CA129134 and RO1-CA137494) and AKW (RO1-CA163863).

References

1. Ernster VL, Ballard-Barbash R, Barlow WE, Zheng Y, Weaver DL, Cutter G, et al. Detection of ductal carcinoma in situ in women undergoing screening mammography. J Natl Cancer Inst. 2002 Oct 16; 94(20):1546–54. [PubMed: 12381707]
2. Virnig BA, Tuttle TM, Shamliyan T, Kane RL. Ductal carcinoma in situ of the breast: a systematic review of incidence, treatment, and outcomes. J Natl Cancer Inst. 2010 Feb 3; 102(3):170–8. Epub 2010/01/15. eng. [PubMed: 20071685]
3. Betsill WL Jr, Rosen PP, Lieberman PH, Robbins GF. Intraductal carcinoma. Long-term follow-up after treatment by biopsy alone. Jama. 1978 May 5; 239(18):1863–7. [PubMed: 205686]
4. Carlson RW, Allred DC, Anderson BO, Burstein HJ, Carter WB, Edge SB, et al. Breast cancer. Clinical practice guidelines in oncology. J Natl Compr Canc Netw. 2009 Feb; 7(2):122–92. eng. [PubMed: 19200416]
5. Schnitt SJ. Local outcomes in ductal carcinoma in situ based on patient and tumor characteristics. J Natl Cancer Inst Monogr. 2010; (41):158–61. Epub 2010/10/20. eng. [PubMed: 20956823]
6. Allegra CJ, Aberle DR, Ganschow P, Hahn SM, Lee CN, Millon-Underwood S, et al. National Institutes of Health State-of-the-Science Conference statement: Diagnosis and Management of Ductal Carcinoma In Situ September 22-24, 2009. J Natl Cancer Inst. Feb 3; 102(3):161–9. eng. [PubMed: 20071686]
7. Jones JL. Overdiagnosis and overtreatment of breast cancer: progression of ductal carcinoma in situ: the pathological perspective. Breast Cancer Res. 2006; 8(2):204. [PubMed: 16677423]
8. Romero L, Klein L, Ye W, Holmes D, Soni R, Silberman H, et al. Outcome after invasive recurrence in patients with ductal carcinoma in situ of the breast. Am J Surg. 2004 Oct; 188(4):371–6. [PubMed: 15474428]
9. Kerlikowske K, Molinaro A, Cha I, Ljung BM, Ernster VL, Stewart K, et al. Characteristics associated with recurrence among women with ductal carcinoma in situ treated by lumpectomy. J Natl Cancer Inst. 2003 Nov 19; 95(22):1692–702. [PubMed: 14625260]
10. Knudsen ES, Ertel A, Davicioni E, Kline J, Schwartz GF, Witkiewicz AK. Progression of ductal carcinoma in situ to invasive breast cancer is associated with gene expression programs of EMT

and myoepithelia. Breast Cancer Res Treat. 2011 Jun; 133(3):1009–24. Epub 2011/12/03. eng. [PubMed: 22134623]

11. Lee S, Stewart S, Nagtegaal I, Luo J, Wu Y, Colditz G, et al. Differentially expressed genes regulating the progression of ductal carcinoma in situ to invasive breast cancer. Cancer research. 2012 Sep 1; 72(17):4574–86. [PubMed: 22751464]
12. Franke WW. Discovering the molecular components of intercellular junctions--a historical view. Cold Spring Harb Perspect Biol. 2009 Sep.1(3):a003061. [PubMed: 20066111]
13. Zhurinsky J, Shtutman M, Ben-Ze'ev A. Plakoglobin and beta-catenin: protein interactions, regulation and biological roles. J Cell Sci. 2000 Sep; 113(Pt 18):3127–39. [PubMed: 10954412]
14. Wheelock MJ, Johnson KR. Cadherins as modulators of cellular phenotype. Annu Rev Cell Dev Biol. 2003; 19:207–35. [PubMed: 14570569]
15. Rodriguez-Boulan E, Nelson WJ. Morphogenesis of the polarized epithelial cell phenotype. Science. 1989 Aug 18; 245(4919):718–25. [PubMed: 2672330]
16. O'Brien LE, Zegers MM, Mostov KE. Opinion: Building epithelial architecture: insights from three-dimensional culture models. Nat Rev Mol Cell Biol. 2002 Jul; 3(7):531–7. [PubMed: 12094219]
17. Kim YS, Won YS, Park KS, Song BJ, Kim JS, Oh SJ, et al. Prognostic significance of HER2 gene amplification according to stage of breast cancer. J Korean Med Sci. 2008 Jun; 23(3):414–20. [PubMed: 18583876]
18. Ross JS, Slodkowska EA, Symmans WF, Pusztai L, Ravdin PM, Hortobagyi GN. The HER-2 receptor and breast cancer: ten years of targeted anti-HER-2 therapy and personalized medicine. Oncologist. 2009 Apr; 14(4):320–68. [PubMed: 19346299]
19. Slamon DJ, Clark GM, Wong SG, Levin WJ, Ullrich A, McGuire WL. Human breast cancer: correlation of relapse and survival with amplification of the HER-2/neu oncogene. Science. 1987 Jan 9; 235(4785):177–82. eng. [PubMed: 3798106]
20. Allred DC, Clark GM, Molina R, Tandon AK, Schnitt SJ, Gilchrist KW, et al. Overexpression of HER-2/neu and its relationship with other prognostic factors change during the progression of in situ to invasive breast cancer. Hum Pathol. 1992 Sep; 23(9):974–9. eng. [PubMed: 1355464]
21. Hoque A, Sneige N, Sahin AA, Menter DG, Bacus JW, Hortobagyi GN, et al. Her-2/neu gene amplification in ductal carcinoma in situ of the breast. Cancer Epidemiol Biomarkers Prev. 2002 Jun; 11(6):587–90. eng. [PubMed: 12050101]
22. Muthuswamy SK, Li D, Lelievre S, Bissell MJ, Brugge JS. ErbB2, but not ErbB1, reinitiates proliferation and induces luminal repopulation in epithelial acini. Nat Cell Biol. 2001 Sep; 3(9): 785–92. eng. [PubMed: 11533657]
23. Wu M, Jung L, Cooper AB, Fleet C, Chen L, Breault L, et al. Dissecting genetic requirements of human breast tumorigenesis in a tissue transgenic model of human breast cancer in mice. Proc Natl Acad Sci U S A. 2009 Apr 28; 106(17):7022–7. eng. [PubMed: 19369208]
24. Kerlikowske K, Molinaro AM, Gauthier ML, Berman HK, Waldman F, Bennington J, et al. Biomarker expression and risk of subsequent tumors after initial ductal carcinoma in situ diagnosis. J Natl Cancer Inst. 2010 May 5; 102(9):627–37. eng. [PubMed: 20427430]
25. Gauthier ML, Berman HK, Miller C, Kozakeiwicz K, Chew K, Moore D, et al. Abrogated response to cellular stress identifies DCIS associated with subsequent tumor events and defines basal-like breast tumors. Cancer Cell. 2007 Nov; 12(5):479–91. eng. [PubMed: 17996651]
26. Witkiewicz AK, Rivadeneira DB, Ertel A, Kline J, Hyslop T, Schwartz GF, et al. Association of RB/p16-Pathway Perturbations with DCIS Recurrence Dependence on Tumor versus Tissue Microenvironment. Am J Pathol. 2010 Sep; 179(3):1171–8. eng. [PubMed: 21756866]
27. Knudsen ES, Pajak TF, Qeenan M, McClendon AK, Armon BD, Schwartz GF, et al. Retinoblastoma and phosphate and tensin homolog tumor suppressors: impact on ductal carcinoma in situ progression. Journal of the National Cancer Institute. 2012 Dec 5; 104(23):1825–36. [PubMed: 23197489]
28. Knudsen ES, Knudsen KE. Tailoring to RB: tumour suppressor status and therapeutic response. Nat Rev Cancer. 2008 Sep; 8(9):714–24. eng. [PubMed: 19143056]
29. Cobrinik D. Pocket proteins and cell cycle control. Oncogene. 2005 Apr 18; 24(17):2796–809. [PubMed: 15838516]

30. Jiang Z, Deng T, Jones R, Li H, Herschkowitz JI, Liu JC, et al. Rb deletion in mouse mammary progenitors induces luminal-B or basal-like/EMT tumor subtypes depending on p53 status. J Clin Invest. 2010 Sep 1; 120(9):3296–309. eng. [PubMed: 20679727]

31. Herschkowitz JI, He X, Fan C, Perou CM. The functional loss of the retinoblastoma tumour suppressor is a common event in basal-like and luminal B breast carcinomas. Breast Cancer Res. 2008 Sep 9.10(5):R75. Epub 2008/09/11. Eng. [PubMed: 18782450]

32. Debnath J, Muthuswamy SK, Brugge JS. Morphogenesis and oncogenesis of MCF-10A mammary epithelial acini grown in three-dimensional basement membrane cultures. Methods. 2003 Jul; 30(3):256–68. Epub 2003/06/12. eng. [PubMed: 12798140]

33. Hebner C, Weaver VM, Debnath J. Modeling morphogenesis and oncogenesis in three-dimensional breast epithelial cultures. Annu Rev Pathol. 2008; 3:313–39. [PubMed: 18039125]

34. Kenny PA, Lee GY, Myers CA, Neve RM, Semeiks JR, Spellman PT, et al. The morphologies of breast cancer cell lines in three-dimensional assays correlate with their profiles of gene expression. Mol Oncol. 2007 Jun; 1(1):84–96. Epub 2008/06/03. eng. [PubMed: 18516279]

35. Taube JH, Herschkowitz JI, Komurov K, Zhou AY, Gupta S, Yang J, et al. Core epithelial-to-mesenchymal transition interactome gene-expression signature is associated with claudin-low and metaplastic breast cancer subtypes. Proc Natl Acad Sci U S A. 2010 Aug 31; 107(35):15449–54. eng. [PubMed: 20713713]

36. Petersen OW, Ronnov-Jessen L, Howlett AR, Bissell MJ. Interaction with basement membrane serves to rapidly distinguish growth and differentiation pattern of normal and malignant human breast epithelial cells. Proc Natl Acad Sci U S A. 1992 Oct 1; 89(19):9064–8. [PubMed: 1384042]

37. Toogood PL, Harvey PJ, Repine JT, Sheehan DJ, VanderWel SN, Zhou H, et al. Discovery of a potent and selective inhibitor of cyclin-dependent kinase 4/6. J Med Chem. 2005 Apr 7; 48(7): 2388–406. [PubMed: 15801831]

38. Fry DW, Harvey PJ, Keller PR, Elliott WL, Meade M, Trachet E, et al. Specific inhibition of cyclin-dependent kinase 4/6 by PD 0332991 and associated antitumor activity in human tumor xenografts. Mol Cancer Ther. 2004 Nov; 3(11):1427–38. [PubMed: 15542782]

39. Dean JL, Thangavel C, McClendon AK, Reed CA, Knudsen ES. Therapeutic CDK4/6 inhibition in breast cancer: key mechanisms of response and failure. Oncogene. 2010 Jul 15; 29(28):4018–32. eng. [PubMed: 20473330]

40. Zajchowski DA, Bartholdi MF, Gong Y, Webster L, Liu HL, Munishkin A, et al. Identification of gene expression profiles that predict the aggressive behavior of breast cancer cells. Cancer Res. 2001 Jul 1; 61(13):5168–78. [PubMed: 11431356]

41. Rakovitch E, Nofech-Mozes S, Hanna W, Narod S, Thiruchelvam D, Saskin R, et al. HER2/neu and Ki-67 expression predict non-invasive recurrence following breast-conserving therapy for ductal carcinoma in situ. British journal of cancer. 2012 Mar 13; 106(6):1160–5. [PubMed: 22361634]

42. Correa C, McGale P, Taylor C, Wang Y, Clarke M, Davies C, et al. Overview of the randomized trials of radiotherapy in ductal carcinoma in situ of the breast. J Natl Cancer Inst Monogr. 2010; (41):162–77. Epub 2010/10/20. eng. [PubMed: 20956824]

43. Erbas B, Provenzano E, Armes J, Gertig D. The natural history of ductal carcinoma in situ of the breast: a review. Breast Cancer Res Treat. 2006 May; 97(2):135–44. Epub 2005/12/02. eng. [PubMed: 16319971]

44. Leonard GD, Swain SM. Ductal carcinoma in situ, complexities and challenges. Journal of the National Cancer Institute. 2004 Jun 16; 96(12):906–20. eng. [PubMed: 15199110]

45. Hanahan D, Weinberg RA. Hallmarks of cancer: the next generation. Cell. 2012 Mar 4; 144(5): 646–74. [PubMed: 21376230]

46. Cavallaro U, Christofori G. Cell adhesion and signalling by cadherins and Ig-CAMs in cancer. Nat Rev Cancer. 2004 Feb; 4(2):118–32. [PubMed: 14964308]

47. Knudsen ES, Ertel A, Davicioni E, Kline J, Schwartz GF, Witkiewicz AK. Progression of ductal carcinoma in situ to invasive breast cancer is associated with gene expression programs of EMT and myoepithelia. Breast Cancer Res Treat. 2011 Dec 2. Epub 2011/12/03. Eng. [PubMed: 22134623]

48. Sutherland RL, Musgrove EA. Cyclins and breast cancer. J Mammary Gland Biol Neoplasia. 2004 Jan; 9(1):95–104. [PubMed: 15082921]

49. Rivadeneira DB, Mayhew CN, Thangavel C, Sotillo E, Reed CA, Grana X, et al. Proliferative suppression by CDK4/6 inhibition: complex function of the retinoblastoma pathway in liver tissue and hepatoma cells. Gastroenterology. 2010 May; 138(5):1920–30. [PubMed: 20100483]

50. Thangavel C, Dean JL, Ertel A, Knudsen KE, Aldaz CM, Witkiewicz AK, et al. Therapeutically activating RB: reestablishing cell cycle control in endocrine therapy-resistant breast cancer. Endocr Relat Cancer. 2011; 18(3):333–45. eng. [PubMed: 21367843]

51. Knudsen ES, Buckmaster C, Chen TT, Feramisco JR, Wang JY. Inhibition of DNA synthesis by RB: effects on G1/S transition and S-phase progression. Genes Dev. 1998 Aug 1; 12(15):2278–92. [PubMed: 9694794]

52. Sotgia F, Williams TM, Schubert W, Medina F, Minetti C, Pestell RG, et al. Caveolin-1 deficiency (-/-) conveys premalignant alterations in mammary epithelia, with abnormal lumen formation, growth factor independence, and cell invasiveness. Am J Pathol. 2006 Jan; 168(1):292–309. Epub 2006/01/10. eng. [PubMed: 16400031]

53. Storey JD. A direct approach to false discovery rates. Journal of the Royal Statistical Society: Series B (Statistical Methodology). 2002; 64(3):479–98.

54. Hackstadt AJ, Hess AM. Filtering for increased power for microarray data analysis. BMC Bioinformatics. 2009; 10:11. Epub 2009/01/10. eng. [PubMed: 19133141]

55. Subramanian A, Tamayo P, Mootha VK, Mukherjee S, Ebert BL, Gillette MA, et al. Gene set enrichment analysis: a knowledge-based approach for interpreting genome-wide expression profiles. Proc Natl Acad Sci U S A. 2005 Oct 25; 102(43):15545–50. [PubMed: 16199517]

56. McClendon AK, Dean JL, Ertel A, Fu Z, Rivadeneira DB, Reed CA, et al. RB and p53 cooperate to prevent liver tumorigenesis in response to tissue damage. Gastroenterology. 2011 Oct; 141(4): 1439–50. [PubMed: 21704587]

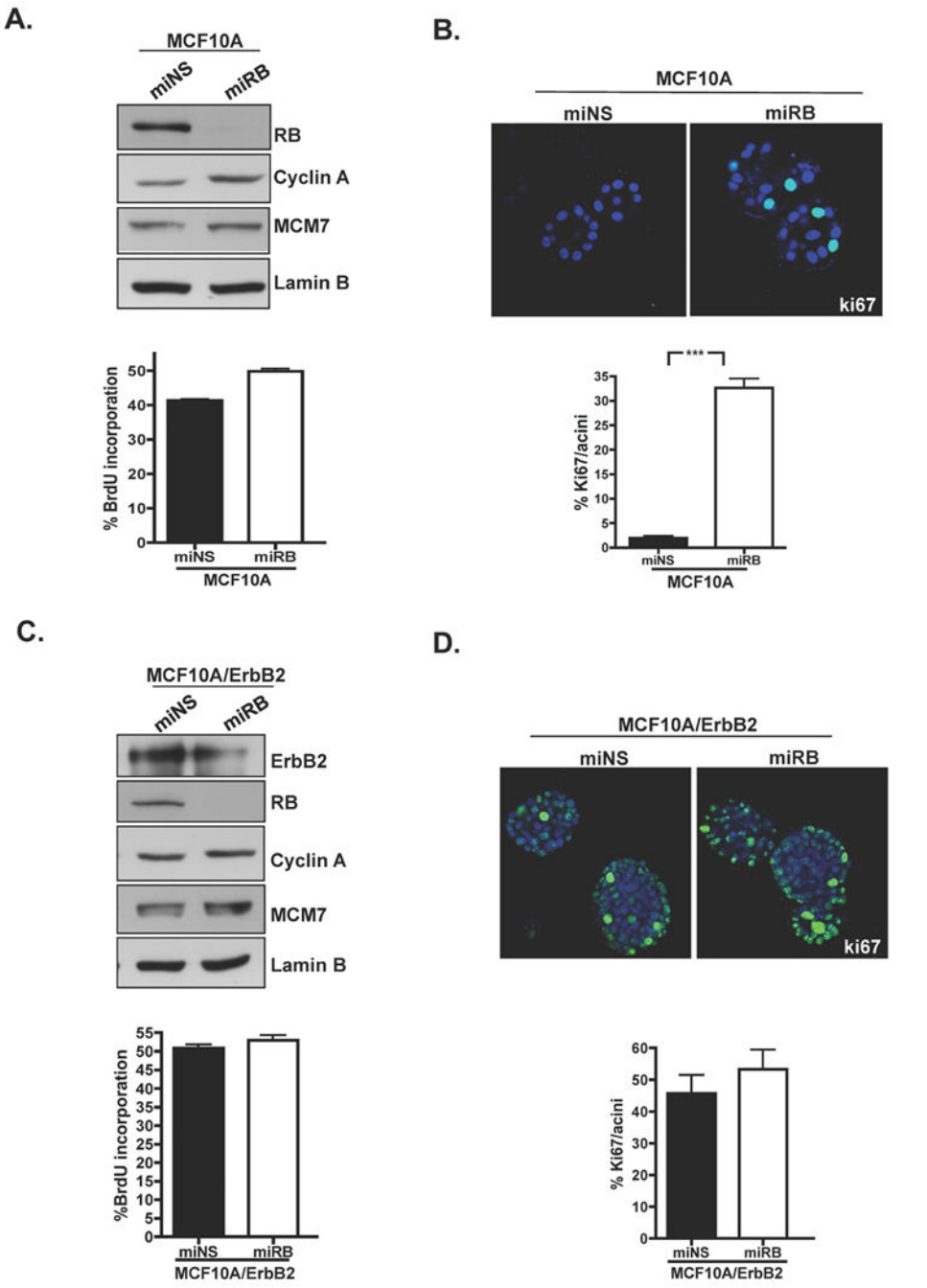

Figure 1. RB-deficient or ErbB2 over expression promotes bypass of acini growth arrest

(A) Cells stably expressing miRB or miNS were analyzed by immunoblot for the indicated proteins *(top panel)*. BrdU incorporation was analyzed by bivariate flow cytometry and data are the average of at least three independent experiments; *bars*, SD *(bottom panel)*. **(B)** Ki67 staining (green) on 10 day acini, (40X) and Ki67 quantification from at least three independent experiments scoring a minimum of 20 acinus; *bars*, SD (***$P < .0001$). **(C)** Cells were infected with ErbB2 lentivirus and subsequently infected with miRB or miNS retroviruses. Cells were harvested and cell lysates were analyzed by immunoblot for the

indicated proteins *(top panel)*. BrdU incorporation was analyzed by bivariate flow cytometry and data are the average of at least three independent experiments; *bars*, SD *(bottom panel)*. **(D)** Ki67 staining (green) on 10 day acini (40X) and Ki67 quantification from at least three independent experiments scoring a minimum of 20 acinus; *bars*, SD.

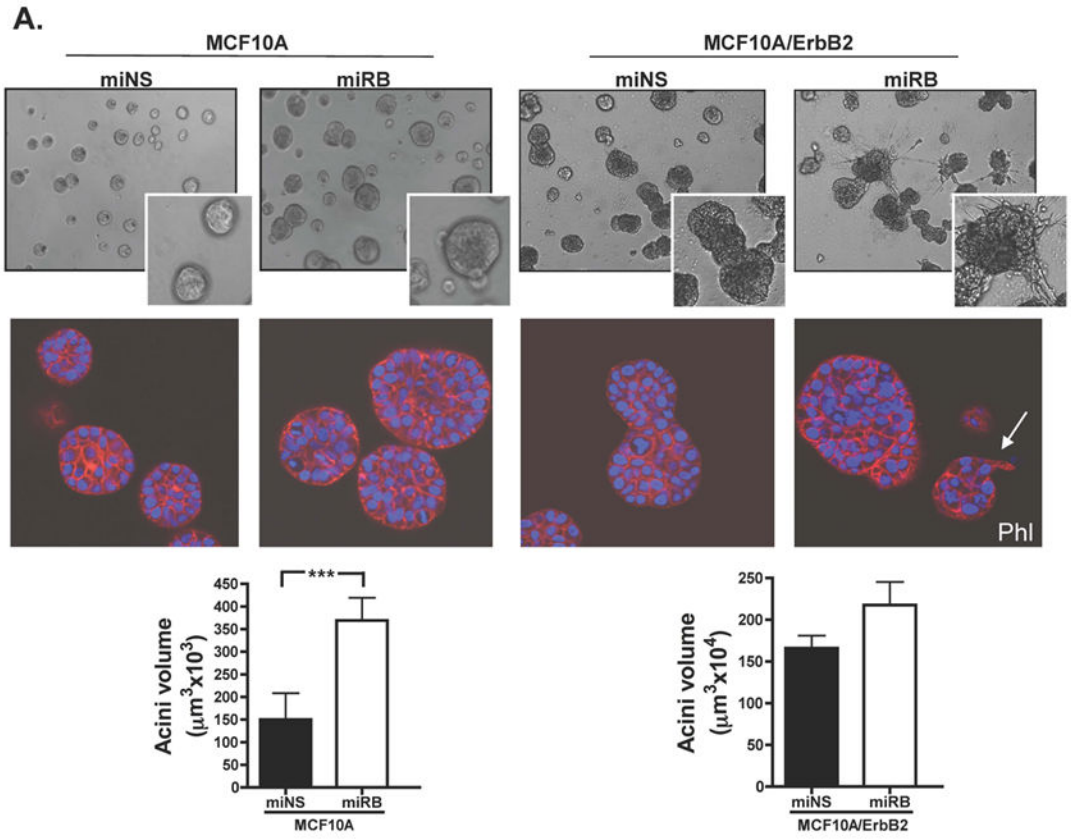

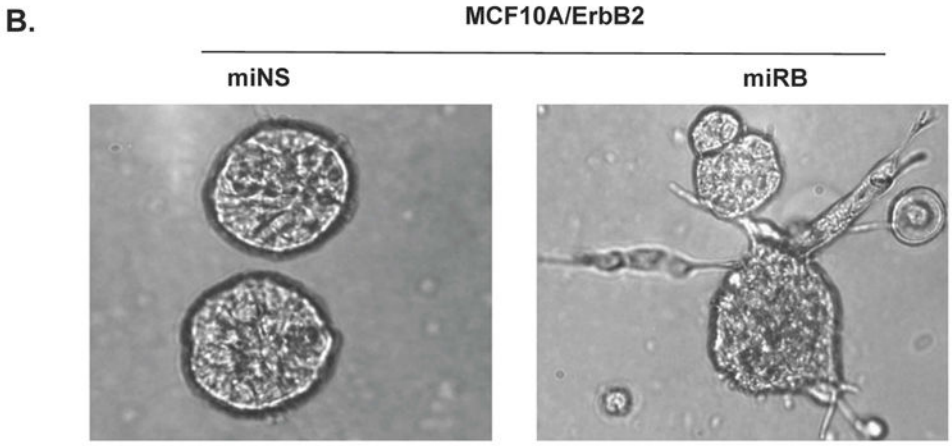

C.

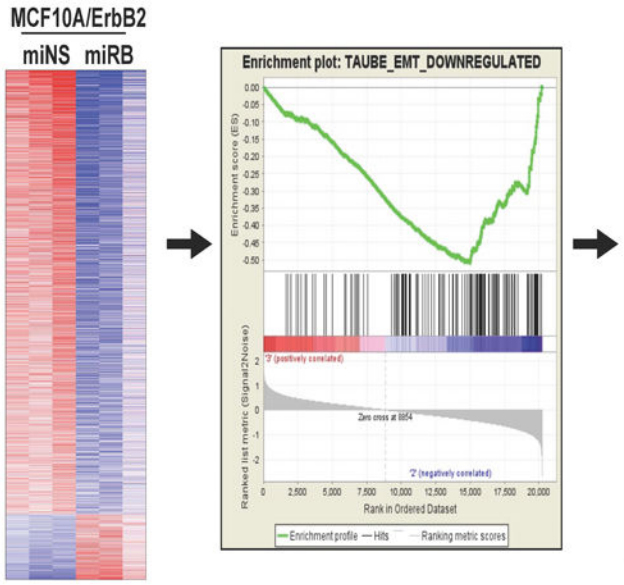

GENE	FOLD CHANGE	P-VALUE
KRT18	-1.85	0.020
KRT15	-1.61	0.027
KRT17	-2.68	0.053
JUP	-3.60	0.003
DSG1	-2.81	0.034
SFN	-282	0.0003
ITGB4	-2.14	0.041
TRIM29	-3.28	0.025
STAP2	-2.32	0.019
AP1M2	-1.77	0.017

Figure 2. Combined effect of ErbB2- and RB-pathway deregulation on acinar morphology

(A) Phase contrast images of acini (10X) were used to measure acini diameters and > 50 acini were scored for each genotype; *bars*, SD (****P* < *.0001*) Phalloidin staining (red) was performed on acini grown for 10days (40x). **(B)** Phase contrast images of acini (20X) were used to visualize stellate acinar structures. Representative images are shown. **(C)** Gene expression data comparing MCF10A/ErbB2 miNS and MCF10A/ErbB2 miRB grown in 3D cultures. Changes in gene expression are displayed as a heat map *(left panel)*. GSEA associated with the Taube-EMT signature *(middle panel) and r*epresentative genes with corresponding fold change and *P*-values are highlighted *(right panel).*

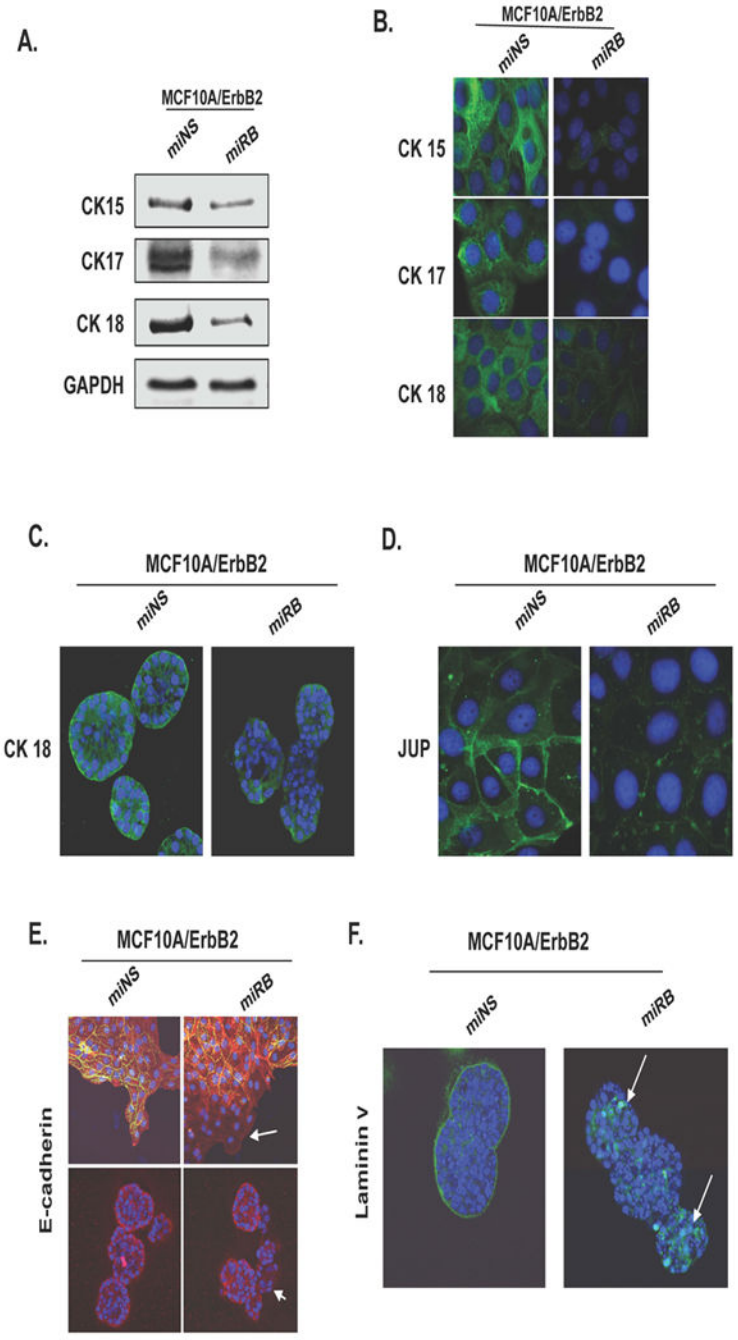

Figure 3. RB loss compromises the integrity of cell-cell adhesion complexes

(A) Immunoblot analysis of MCF10A ErbB2 cells either transduced with miNS or miRB are shown for the indicated proteins. **(B)** Representative images of cells in 2D cultured stained for the indicated cytokeratins. **(C)** Representative images of CK18 stained in 3D cultures. **(D)** Representative images of cells in 2D stained for junctional plakoglobin (JUP). **(E)** Representative images of cell in 2D cultured stained for E-cadherin (green) and Phalloidin (red) *(top panel) and* acini stained for E-cadherin (red*)* are shown. Leading edges of RB-

deficient cells displaying decreased E-cadherin expression are highlighted *(arrows, bottom panel)*. **(F)** Representative images for Laminin V in 3D cultures.

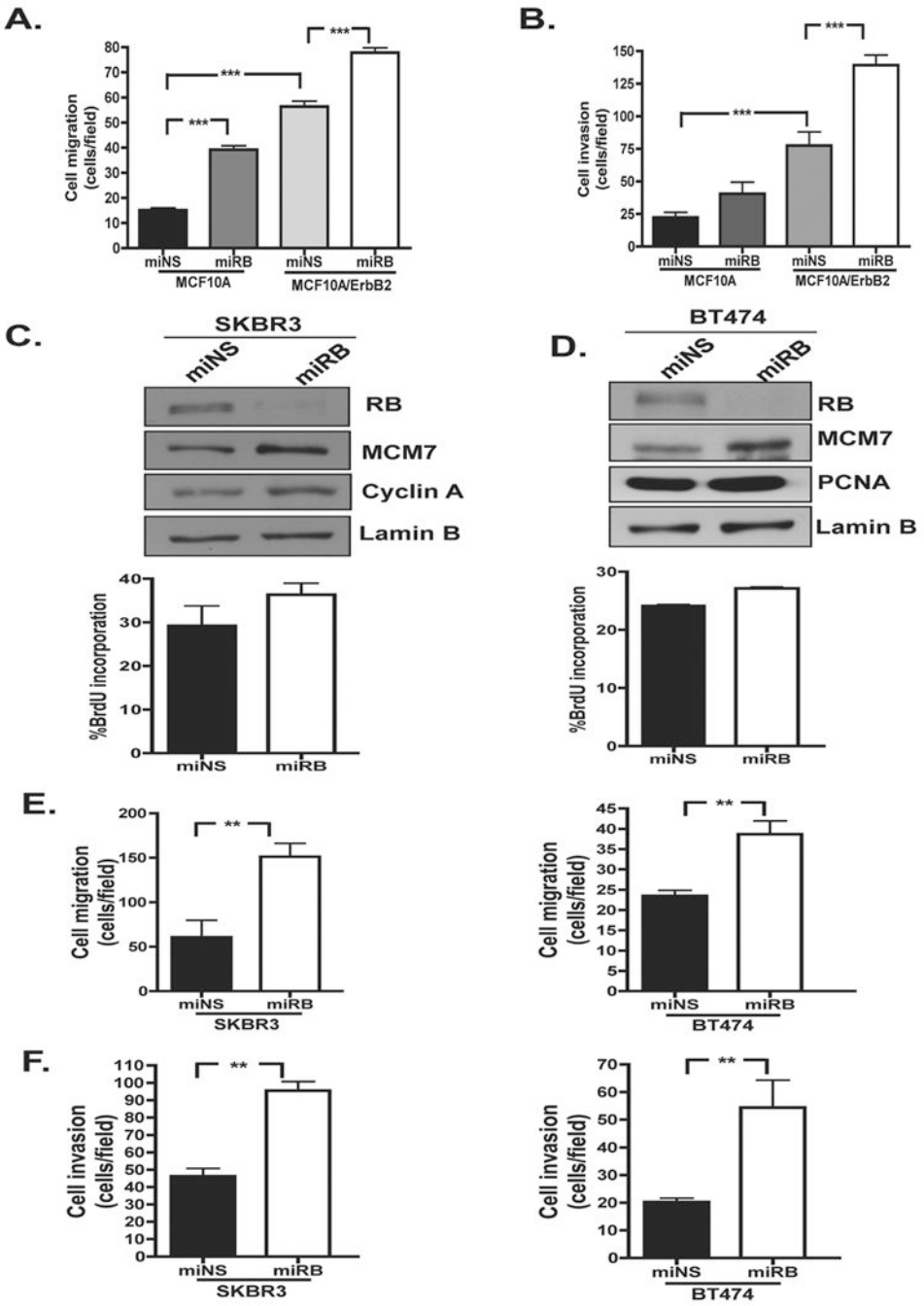

Figure 4. RB loss promotes cell migration and invasion in ErbB2 over expressing cells

(A) Cell migration and **(B)** cell invasion of MCF10A cells harboring ErbB2 over expression and/or RB-deficiency by Boyden Chamber assays; *bars*, SD. (***$P < .0001$) **(C/D)** SKBR3 and BT474 cells transduced with miRB or miNS retroviruses. Cells were harvested and cell lysates were analyzed by immunoblot for the indicated proteins. BrdU incorporation was analyzed by bivariate flow cytometry and data are average of at least three independent experiments; *bars*, SD. **(E/F)** Analysis of SKBR3 miNS/miRB and BT474 miNS/miRB cell migration by Boyden Chamber assays; *bars*, SD. (**$P<0.01$) **(F)** Analysis of SKBR3 miNS/

miRB and BT474 miNS/miRB cell invasion by Boyden Chamber assays; *bars*, SD. (***P<0.01).*

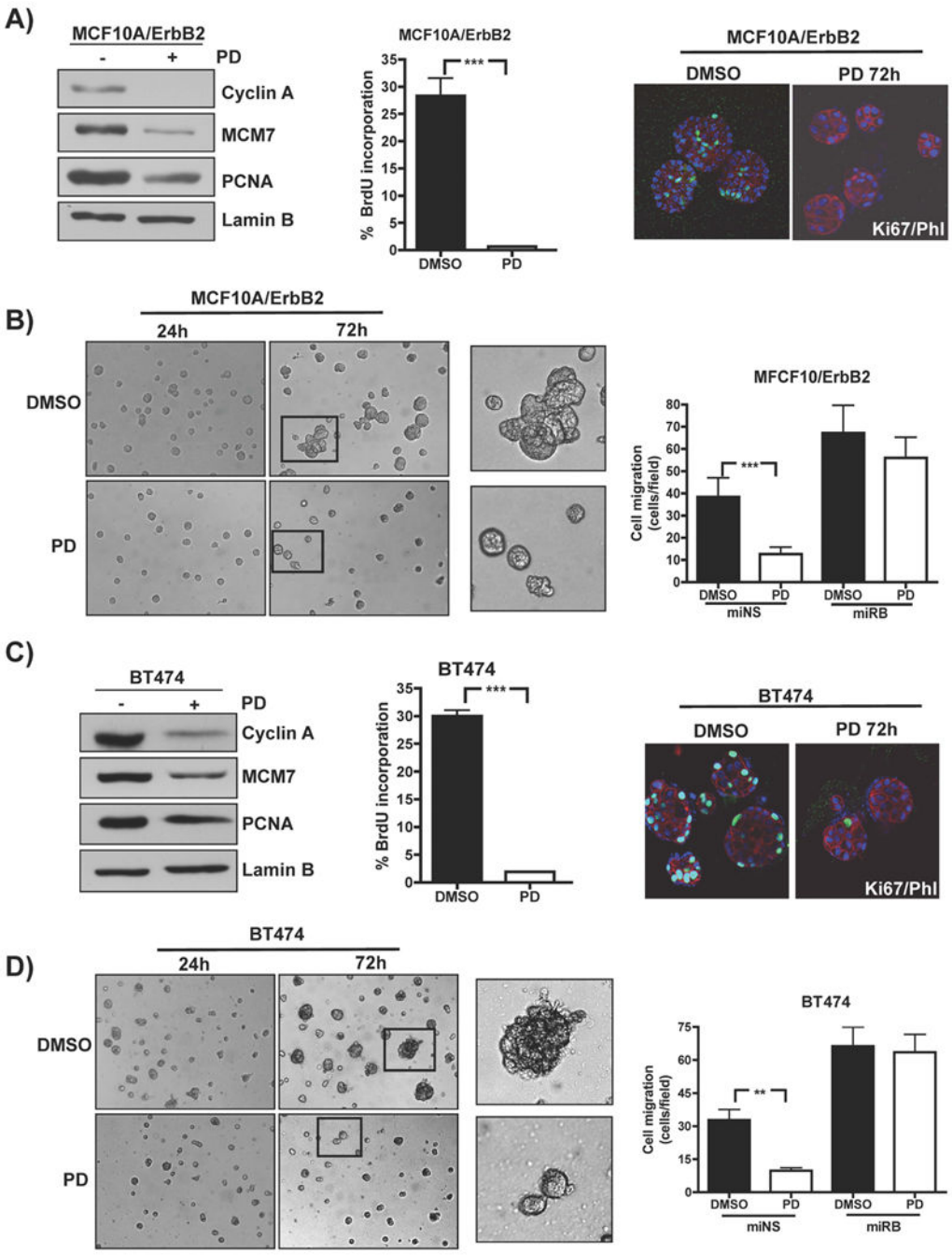

Figure 5. Activation of the RB pathway prevents abnormal multi-acini growth and cell invasion

(A) RB-proficient MCF10A/ErbB2 cells were treated with 0.5μM PD-0332991 for 24h. Cells were harvested and cell lysates were analyzed by immunoblot for the indicated proteins *(left panel)*. BrdU incorporation was analyzed by bivariate flow cytometry and data are the average of at least three independent experiments; *bars*, SD (***$P < .0001$) *(middle panel)*. Ki67 and phalloidin co-staining of MCF10A/ErbB2 acini treated with 0.5μM PD-0332991 for 72h (20X) *(right panel)*. **(B)** RB-proficient MCF10A/ErbB2 cells grown in 3D culture and treated with 0.5μM PD0332991 for 72h, (20X) *(left panel)*. Analysis of cell

migration by Boyden Chamber assays supplemented with 0.5μM PD0332991 was performed; *bars*, SD. (**$P=.003$) *(right panel)*. **(C)** RB-proficient BT474 cells were treated with PD-0332991 and analyzed by immunoblotting, BrdU incorporation and proliferation in 3D culture. BrdU incorporation data are the average of at least three independent experiments; *bars*, SD (***$P < .0001$). **(D)** RB-proficient BT474 cells were treated for growth in 3D culture and cell migration. Migration data are the average of at least three independent experiments; *bars*, SD (**$P < 0.0037$).

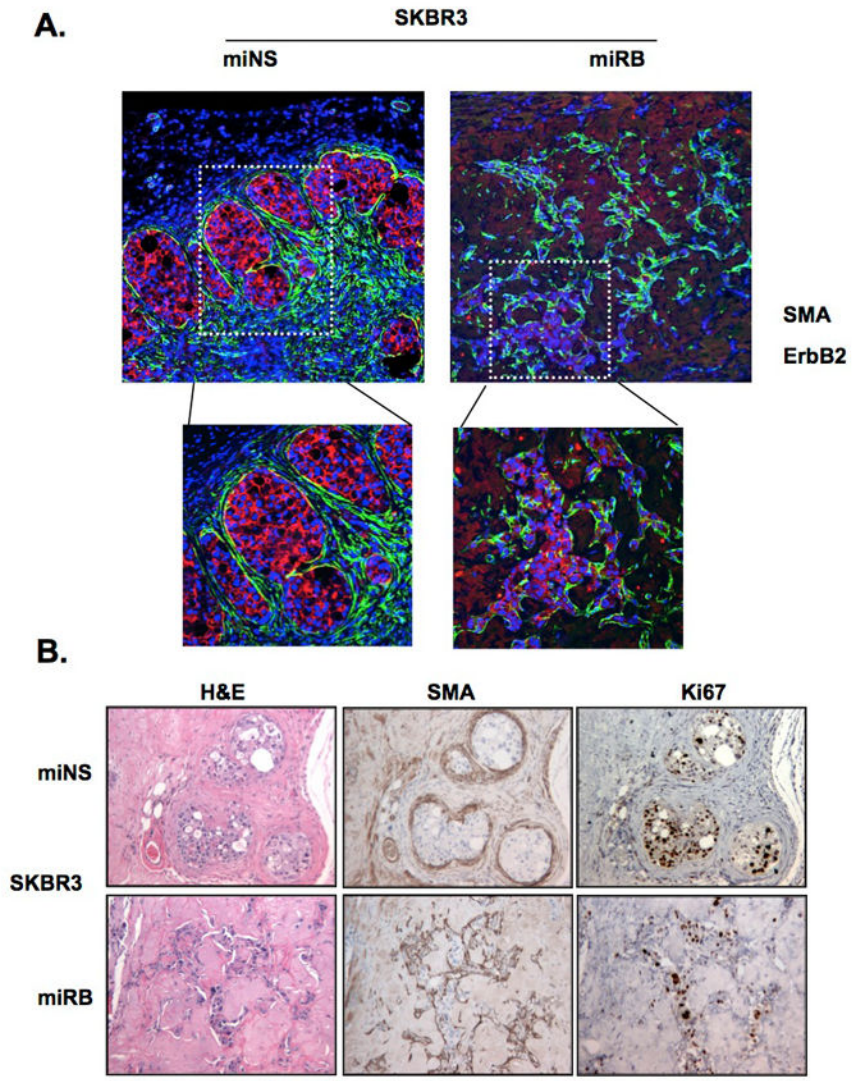

Lesions observed	SKBR3 miNS n=15	SKBR3 miRB n=15
DCIS lesions >2	71.5%	20%
DCIS lesions >10	28.5%	0.0%
Invasive lesions	0.0%	80%

Figure 6. RB plays a role in preventing invasive tumor growth in vivo

(A) Dual staining for ErbB2 (red) and SMA (green) in SKBR3 miNS and SKBR3 miRB injected mammary glands. **(B)** Representative H&E, Smooth muscle actin (SMA) and Ki67 staining in SKBR3 miNS and SKBR3 miRB lesions are shown *(left panels)*. Table depicting percentage of DCIS and invasive lesions from SKBR3 miNS and SKBR3 miRB orthotopic injections (n=15) *(right panel)*

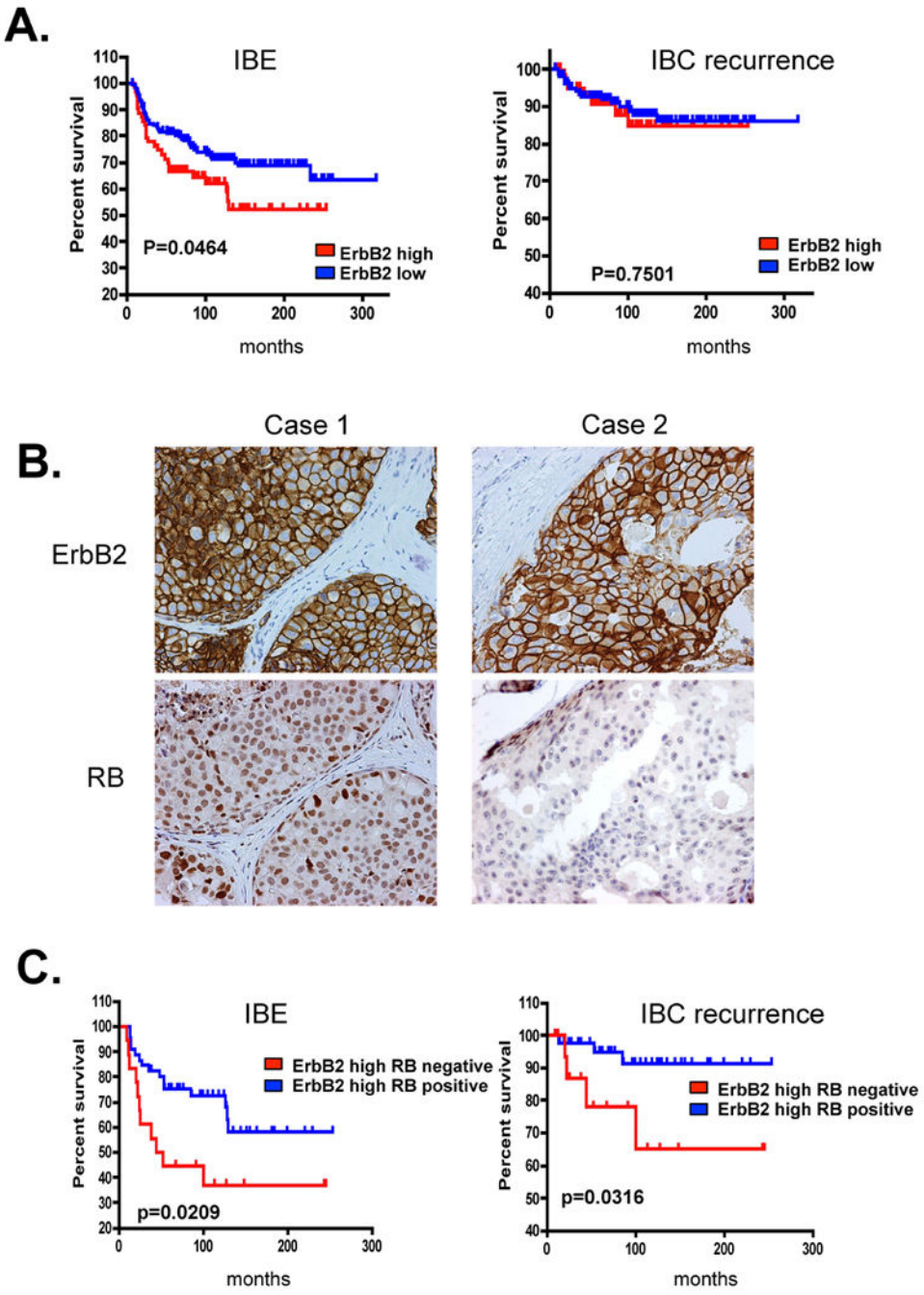

Figure 7. RB deficiency is associated with increased disease progression in DCIS

(A) ErbB2 high (3+) status was compared against all other ErbB2 staining (0, 1+, 2+) for any recurrent disease (ipsilateral breast event) or invasive progression using Kaplan-Meier analysis. ErbB2 high was associated with risk of a subsequent ipsilateral breast event, but not progression to invasive disease. **(B)** Representative images of RB staining in DCIS lesions cases with high ErbB2. **(C)** ErbB2 high (3+) cases were stratified by RB status

(positive vs. negative). Cases with RB loss in this subtype were associated with both risk of a subsequent ipsilateral breast event and progression to invasive disease.